

## Residence time distribution (RTD) model of water flooding in vertical sand column using Technetium-99m as the radiotracer

<sup>a</sup> Noraishah Othman \*, <sup>b</sup> Nini Syaheera Jasni, <sup>b</sup> Nor Roslina Rosli, <sup>a</sup> Nazrul Hizam Yusof, <sup>a</sup> Mohamad Rabaie Shari, <sup>a</sup> Hearie Hassan, <sup>a</sup> Airwan Affandi Mahmood, <sup>a</sup> Ainul Mardhiah Terry, <sup>a</sup> Nurliyana Abdullah

<sup>a</sup>Plant Assessment Technology (PAT), Industrial Technology Division, Malaysian Nuclear Agency, Kajang, Selangor

<sup>b</sup>School of Chemical Engineering, College of Engineering, Universiti Teknologi MARA, Selangor, Malaysia

\*Corresponding email: [noraishah@nm.gov.my](mailto:noraishah@nm.gov.my)

### Abstract

Waterflooding is one of the secondary oil recovery methods practised in the oil and gas industry to improve the extraction of residual oil from oil reservoirs. The idea of understanding the behaviour of reservoirs should be explored further so that the appropriate action can be conducted in the targeted area to optimise oil production. Thus, the intervention of a radiotracer is introduced to provide the fluid flow details in a reservoir. In this study, Technetium-99m (Tc-99m) was used for waterflooding activity inside a fabricated sand column. Tc-99m was selected due to its availability and short-lived tracer (6 hours). It also emits gamma rays with an energy of 0.140 MeV. The sand column was compacted with a 150 µm grain size of sand and 5 mL of approximately 3614MBq activity Tc-99m was injected inside the column which was arranged vertically. The Residence time distribution (RTD) model was developed from the results collected at the outlet of the sand column. The RTD model indicated the vertical sand column behaved as a Perfect Mixer in a Parallel (PMP) model and the RTD experiment verified the model well. The experimental RTD showed the existence of channelling that resembles the parallel paths that reduce water flooding efficiency. Moreover, the study also showed that the tracer activity can be as minimum as possible as long as it is detectable for data analysis.

### Article Info

<https://doi.org/10.24191/mjct.v5i2.19758>

#### Article history:

Received date: 15 September 2022

Accepted date: 21 October 2022

Published date: 31 October 2022

#### Keywords:

Waterflooding  
Radiotracer  
Technetium-99m  
RTD model  
Channelling /parallel path

### 1.0 Introduction

Radiotracer technology (RT) has been applied in industries for more than 50 years in plant diagnostic and troubleshooting without plant shutdown (International Atomic Energy Agency, 2008). This technology has been more prevalent in several applications such as determining the dead zone/stagnant zones in wastewater treatment plants (WWTP), measurement of flow rates for the calibration of flowmeter or non-installed flowmeter, determination of leaks in buried pipelines and industrial heat exchangers and last but not least inter-well (IWTT) communication in oilfields (IAEA, 2001, 2004; Othman & Kamarudin, 2014). RT can be performed by injecting a radiotracer at the inlet of the system (injection well) and monitoring it at the outlet (production well). The data output can be treated and analysed to investigate the behaviour of the system. The dynamic flow pattern of fluid in a reservoir can be measured by tagging injection water with a suitable

nuclide. A response curve versus time can be obtained and analysed.

To date, information on the use of radiotracer to determine the Residence time distribution (RTD) model for water flooding activity to improve crude oil recovery is scarce. Only recently, investigations on radiotracer intervention during water flooding in commercial core flood rigs have been carried out. The investigation reported that the radiotracer can provide information on the core flood which enables researchers to improve their parameters for water flooding optimisation (Othman et al., 2020). Hence the motivation of this work is to integrate radiotracer technology into the activities of waterflooding.

Waterflooding is a common secondary recovery oil extraction method that can enhance oil recovery by up to 45 percent of the overall recovery factor. Waterflooding is commonly used due to its availability, cost-effectiveness and simplicity (Danial Azim Che Aziz et al., 2020; Zitha et al., 2011). To evaluate the

effectiveness of the waterflooding, sweep efficiency evaluation should be done. Sweep efficiency experiment has been conducted all around the oil and gas industry. Studies have been done using core flooding, simulation, analytical model or evaluation using substitution index (Al-Shalabi & Sepehrnoori, 2016; Dollah et al., 2018). In this work, radiotracer was utilised to assist in the understanding of its sweep efficiency.

The knowledge of the total/swept efficiency is not a simple task because the reservoirs are underground formations and therefore remote to man and conventional tools (Hamidi & Rafati, 2012; Rahmani et al., 2013). A radiotracer is a tool that accesses and runs across the reservoir, contacting portions of interest and giving information about the total/swept efficiency (Melo & Almeida, 2017). The output from the analysis can be in the form of residence time distribution (RTD) which can represent the fluid flow in the reservoir and be interpreted using RTD models.

## 2.0 Methodology

### 2.1 Material

Two radiotracer experiments have been carried out to investigate the information that can be retrieved from this new approach during the waterflooding study. Technetium-99m (Tc-99m), a metastable nuclear isomer of technetium-99, was used as the radioactive tracer in this study. It is the most used radioisotope in the medical radiopharmaceutical field for the imaging of various parts of internal organs such as the brain, kidney, thyroid, liver, bone, and heart (Mettler & Guiberteau, 2012; Pinkerton et al., 1985; Ranamukhaarachchi et al., 2019; Schölmerich et al., 1988; van der Velden et al., 2019). The metastable isotope is extracted from a decaying sample of molybdenum-99 (99Mo) using a technetium-99m generator, also known as a Moly generator (Rodríguez López et al., 2017; Skuridin et al., 2016). In each experiment, 5 mL of Tc-99m was eluted from a Molybdenum-99 generator to produce a liquid radiotracer.

### 2.2 Experimental setup

The experimental setup to conduct the waterflooding activity is shown in Fig. 1. About 30 cm length of sand column was compacted with 150  $\mu\text{m}$  sand particles and arranged in a vertical position. After that, about 300 mL of prepared formation water was added to the column followed by 200 mL of kerosene as a light oil sample. Upon completion, two Sodium Iodide (NaI) scintillation detectors were arranged at the inlet and outlet of the

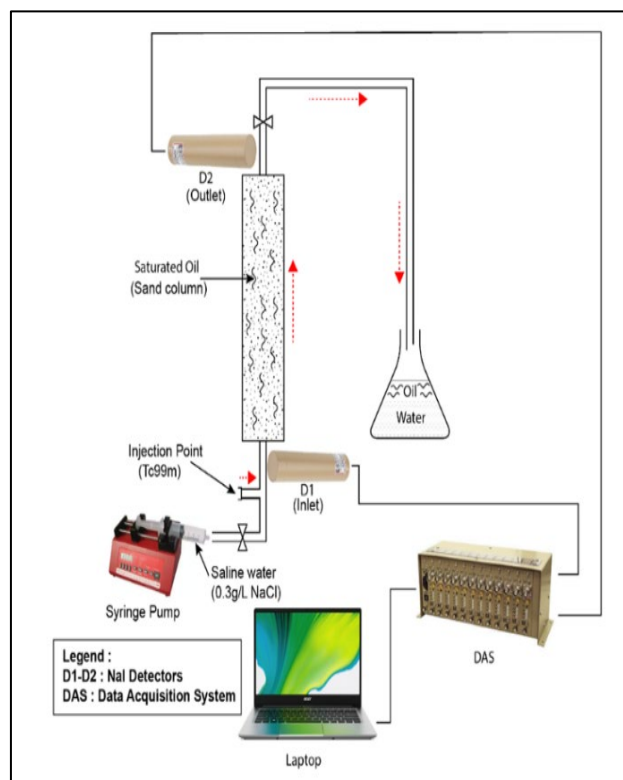


Fig. 1: Schematic diagram of the experimental setup

column, labelled D1 and D2 respectively. These detectors were connected to a Data Acquisition System (DAS) that was attached to a laptop computer for data monitoring and storage. A syringe pump was attached at the upstream of the set-up to supply continuous NaCl saline water (300 ppm) for water flooding activity.

Once the column was saturated and ready for water flooding, 5 mL of the liquid Tc-99m was injected instantaneously. The pump for saline water injection was then turned on to commence waterflooding. The radiation signals were monitored and recorded on the laptop. Finally, the oil recovery and water effluent were collected at the outlet of the column. The experiment ended when the radiation signals approached the background reading. The experiment was repeated for consistency. Table 1 shows the parameters involved in the radiotracer experiments.

### 2.3 Residence time distribution (RTD) Model

Residence time distribution (RTD) is a fundamental parameter in reactor design that provides the time the particles reside in a particular vessel such as a reactor (Bhivgade et al., 2019; Jegede et al., 2019; Menon et al., 2019; Sievers & Stickel, 2018; Wojewódka et al., 2019). It is rich in processing vessel information which enables it to characterise the extent of their deviation from ideal behaviour. The mean residence time (MRT) is the average time that a tracer resides in the system.

The MRT can be calculated using the first moment ( $M_i$ ) in discrete form as shown in Eq. (1). The RTD ( $E(t)$ ) can be calculated using Eq. (2).

$$M_i = \frac{\int_0^\infty t c_i(t) dt}{\int_0^\infty c_i(t) dt} \quad (1)$$

where  $i=1,2,\dots,n$

$$E(t) = \frac{c(t)}{\int_0^\infty c(t) dt} \quad (2)$$

where  $C(t)$  is the concentration of radiotracer monitored by NaI scintillation detectors in counts per second (cps) as the numerator, and the denominator is the area under the curve of plotted  $C(t)$ .

The detected signal is normalised by dividing it by the area under the curve. The RTD models can provide theoretical information or describe the hydrodynamic behaviour of the reactor (IAEA, 2001; International Atomic Energy Agency, 2008).

In 2008, the International Atomic Energy Agency (IAEA) recommended six mathematical models to be used with the RTD experiments. These models are the axial dispersed plug flow model, the axial dispersed plug flow with exchange model, the Perfect Mixers in Series (PMS) model, the PMS with exchange model, the PMP model and the perfect mixers with recycle model respectively. Each model has specific parameters, which are optimised by fitting the model RTD function to the experimental RTD data by the least-squares curve fitting method. The quality of the fit is judged by choosing the model parameters to minimise the sum of square errors (SSE) between the data and the model function (Fazli-Abukheyli & Darvishi, 2019; Lu et al., 2019; Sugiharto et al., 2009). The SSE of the differences between the model and the data are minimised and fulfilled using Eq. (3):

$$\text{Sum of Square (SSE)} = \left[ \frac{1}{N_T} \int_0^\infty [E_{exp}(\theta) - E_m(\theta, N)]^2 d\theta \right]^{1/2} = \text{Minimum} \quad (3)$$

where  $N_T$  is the number of data points,  $E_{exp}(\theta)$  is the experimentally measured curve, and  $E_m(\theta, N)$  is the simulated model.

**Table 1:** Parameter of each experimental setup

Parameters	<sup>99m</sup> Tc (1)	<sup>99m</sup> Tc (2)
Flowrate, Q (mL/min)	3.5	3.5
Saturated oil (mL), $S_{or}$	198	200
Formation water volume, $V_f$ (mL)	335	310
Water flooding volume, $V_w$ (mL)	712	543
Dose rate of <sup>99m</sup> Tc ( $\mu$ Sv/h) @ 1m	120	30

### 3.0 Results and discussion

The results from the replicates of experiments were comparable. The radiotracer activity was determined prior to the waterflooding experiment.

#### 3.1 Radiotracer activity determination

Technetium-99m is a short half-life tracer, with a photopeak of gamma-ray emission of 0.140 MeV, making it a very minimal risk of toxicity. The dose rate of Tc-99m ( $\mu$ Sv/h) at a one meter distance from the source was measured using a portable survey meter (Ludlum model 3) fitted with a pancake-type radiation detector (Model 44-9). The liquid of 5 mL Tc-99m was kept in a vial and it has to be unshielded in order to measure the actual activity of Tc-99m. The activity of Tc-99m at the site can be determined using Eq. (4) with proper unit conversions (Woods, 1982a). Table 2 shows the values of the measured dose rate and the calculated activity.

$$\text{Dose rate} \left( \frac{\mu\text{Sv}}{\text{h}} \right) = \Gamma \left( \mu \frac{\text{Sv}}{\text{h}} / \text{MBq} \right) \times \text{Activity}(\text{mCi}) / r^2 \quad (4)$$

#### 3.2 Waterflooding tracer experiment

The percentage of oil recovery obtained from the waterflood experiment is shown in Table 3. The use of radiotracer (Tc-99m) did not influence the yield of oil.

The raw data obtained from the radiotracer experiment contained statistical fluctuations that needed to be treated prior to RTD determination. The raw data were subjected to treatment steps such as background removal, radioactive decay, starting-point correction, filtering and data extrapolation (Goswami et al., 2020; Kasban et al., 2010, 2016; Othman et al., 2018; Sheoran et al., 2018).

Fig. 2 shows the results of one of the radiotracer experiments after data treatment. The results for the other experiment were very consistent with this result and therefore not discussed in this paper. The injection time and first tracer arrival time (FTA) at the outlet of the column were detected at 100 s and 5800 s, respectively.

**Table 2** Parameters of calculation of activity at site

Parameters	Exp (1)	Exp (2)
Dose rate of Tc-99m ( $\mu$ Sv/h) @ 1m	120	30
Tc-99m $\Gamma$ ( $\mu$ Sv/h/MBq)	0.0332	0.0332
Energy (MeV)	0.140	0.140
Activity of 5mL Tc-99m (MBq)	3614	903
r (distance of 5mL Tc-99m)	1.0	1.0

The long duration taken by the tracer to arrive at FTA, which is approximately 1.6 hours, indicates the struggle the injected water had to overcome in order to emerge at outlet D2. Several possible reasons for the extended time are the flow rate, the resistance due to compact sand and the gravitational force (Chequer et al., 2019; Mora et al., 2016; Sun et al., 2018; Zhong et al., 2020). The 3.5 mL/min was most probably insufficient force to supply water to the whole column during water flooding activity. Although the idea of using the low flow rate was to reduce fingering effects, the vertical arrangements aggravated the waterflooding efficiency. Thus, it was incapable of enhancing the oil recovery. Moreover, the compacted sand has caused difficulties for the water supply to reach the surface, thus it sought the low-pressure area or any cracks to seep through the surface. The water-laden at the bottom has created a pressure build-up and caused the formation of fine cracks from the bottom to the top of the sand column. A significant amount of time was required for the pressure build-up before FTA was achieved. Inevitably, the gravitational force was another major reason for the lengthy time whereby the water flow needs equitable force and ample time to counter the vertical arrangement before reaching the outlet of the column.

Similar findings have been reported in the characteristics of upward seepage flow in sand columns and proposed that different particle shapes and sizes as well as packing porosity contribute to a significant effect on the seepage flow of fluid (Fen et al., 2020; Ma et al., 2019).

Fig. 3 shows the RTD curve after normalisation using Eq. (1). It clearly showed that additional spikes area observed once the radiotracer arrived at the outlet of the column (D2). The spikes are indications of channelling or parallel paths occurring inside the column. These parallel paths have introduced short-circuiting or bypass whereby the liquid radiotracer Tc-99m had found the shortest way to penetrate the surface of the sand column. This phenomenon does not represent the bulk fluid during water flooding activity. Most probably, the bulk fluid of saline water split into smaller volumes that caused a low sweeping volume of residual oil (Fannir et al., 2018; Suekane et al., 2017).

It can be concluded also that the sand pack was not properly packed thus it created weak spots with low pressure. The pressure gradient caused the existence of parallel paths along the vertical column that facilitated the fluid flow. Moreover, the vertical arrangement and low flow rate have added to its casualties. As mentioned

in the previous section, IAEA introduced six RTD models to be fitted to the radiotracer experiment. Nevertheless, in this study, only two RTD models successfully fitted the experimental results. These models are the perfect mixer in series model (PMS) and perfect mixers in parallel model (PMP) as shown in Fig. 4 and 5, respectively.

Comparing between Fig. 4 and 5, both the PMS and PMP models, respectively, appeared very similar to one another. The selection of the best fitted RTD model was then done based upon the minimum value of Error in Sum of Squares (SSE) (Sugiharto et al., 2009). The SSE values are shown in Table 4, which shows that the PMP model has a lower SSE value as compared to the PMS model. Thus, the PMP model was chosen as the best RTD model.

The PMP model simply consists of the association of two series of perfect mixers arranged in parallel. The arrangement of PMP is shown in Fig. 6.

**Table 3:** Results of oil recovery

Parameters	Results Exp 1	Results Exp 2
Saturated oil, $S_{or}$ (mL)	198	200
Recovered oil (mL)	123	118
% Oil recovery	62.1	59.0

**Table 4** Sum of squares error (SSE)

Models	Parameters				SSE	Ranks
	$\tau_1$	$\tau_2$	$J_1$	$J_2$		
Perfect mixer in series Model	771	-	38	-	$1.59 \times 10^{-9}$	2
Perfect mixer in parallel Model	771	39	38	3500	$1.39 \times 10^{-9}$	1

$J$  = number of mixers,  $\tau$  = mean residence time

The first parallel path consists of  $J_1$  and  $Q_1$  for  $V_1$  and the second path comprises of  $J_2$  and  $Q_2$  for  $V_2$  respectively. The total flow rate is denoted as  $Q$ . Where  $J$  is the number of perfect mixers arranged in series for successive parallel paths. Moreover, each parallel path has its own  $\tau$ , mean residence time that represents the Eq. (5):

$$\tau = V/Q \tag{5}$$

where  $V$  is the volume of formation water,  $Q$  is the flowrate of water-flooding (mL/min).

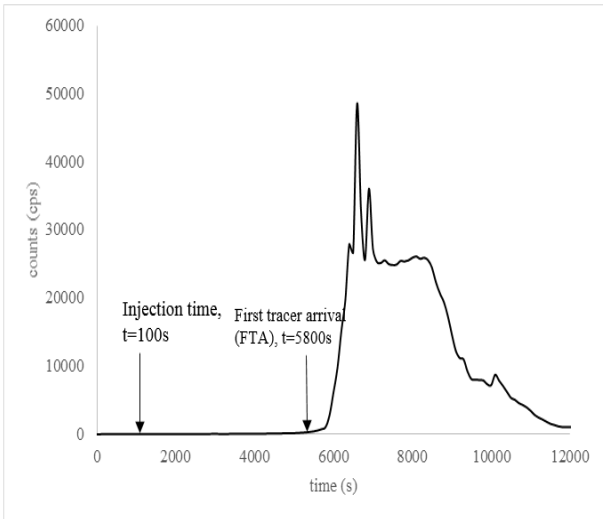


**Fig. 2:** Experimental tracer results at position D2 after data treatment; counts per seconds in cps versus time in seconds (s)

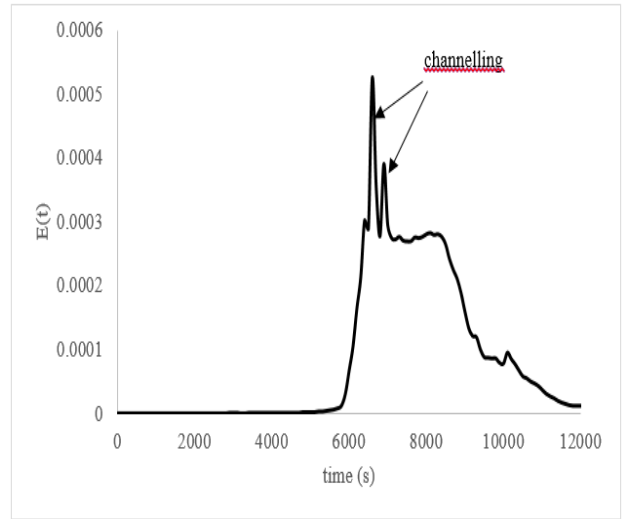


**Fig. 3:** Residence time distribution (RTD)  $E(t)$  curve of the experimental results after normalisation using Eq. 1 at D2; RTD versus time in seconds (s)

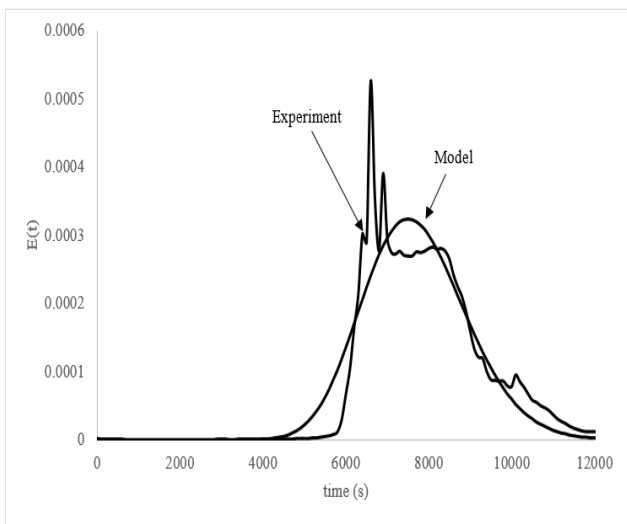


**Fig. 4:** Experimental residence time distribution (RTD) using perfect mixer in series (PMS) model; RTD versus time in seconds (s)

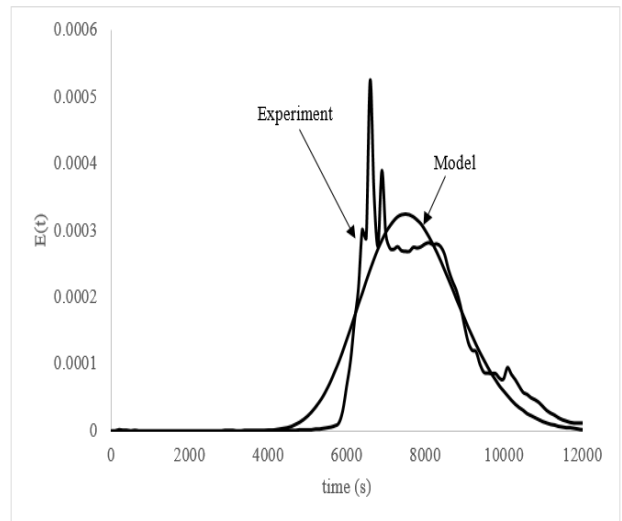


**Fig. 5:** Experimental residence time distribution (RTD) using perfect mixer in parallel (PMP) model; RTD versus time in seconds (s)

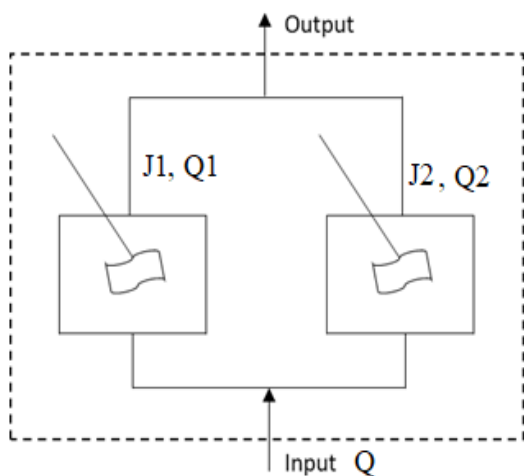


**Fig. 6:** Perfect mixer in parallel (PMP) model diagram

Thus, the mean residence time,  $\tau$  is the average time the particles reside inside the column in minute. In this study, the  $V$  was the volume of formation water which was 335 mL and  $Q$  was 3.5 mL, respectively. Hence, the calculated  $\tau$  was 96 min. The discrepancies of the calculated  $\tau$  to model can be translated to the presence of channelling flow or parallel flow in the column which can be observed from the  $\tau$  obtained from the PMP model as shown in Table 4.

#### 4.0 Conclusions

Several highlights have been discovered in this work. Tc-99m worked wonders as a liquid radiotracer for waterflooding activity. The experimental curves fitted two out of the six RTD models as described by IAEA. Of the two models, the PMP resulted in a slightly lower

SSE value as compared to the PMS. The PMP RTD Model describes the vertical column well.

The results also verified the presence of channelling and parallel paths in the vertical sand column. It can be implied that water flooding did not fully purge the residual oil in bulk instead it splits and fingers into several sections. The vertical arrangement with a slow flow rate even aggravated the oil production since the water supply had to counter the gravitational force. Thus, it is recommended the arrangement be modified to a horizontal position for future works. Finally, the activity of the radiotracer can be as minimum as possible as long as the signals are detectable.

## References

- Al Hadabi, I., Sasaki, K., Sugai, Y., & Kano, N. (2022, March 21–23). *The effects of kaolinite fine particles in sandstone reservoir on Omani medium oil recovery by low-salinity water flooding*. [Paper presentation]. 2022 SPE Conference at Oman Petroleum & Energy Show, Muscat, Oman. <https://doi.org/10.2118/200253-MS>.
- Al-Shalabi, E. W., & Sepehrnoori, K. (2016). A comprehensive review of low salinity/engineered water injections and their applications in sandstone and carbonate rocks. *Journal of Petroleum Science and Engineering*, 139, 137–161. <https://doi.org/10.1016/j.petrol.2015.11.027>
- Bhivgade, U., Maralla, Y., Bhanvase, B. A., & Sonawane, S. (2019). Hydrodynamic, Mass Transfer and RTD Studies of Fluid Flow in a Spiral Microreactor. *Journal of The Institution of Engineers (India): Series E*, 100(2), 139–146. <https://doi.org/10.1007/s40034-019-00143-3>
- Chequer, L., Al-Shuaili, K., Genolet, L., Behr, A., Kowollik, P., Zeinijahromi, A., & Bedrikovetsky, P. (2019). Optimal slug size for enhanced recovery by low-salinity waterflooding due to fines migration. *Journal of Petroleum Science and Engineering*, 177, 766–785. <https://doi.org/10.1016/j.petrol.2019.02.079>
- Dollah, A., Rashid, Z. Z., Othman, N. H., Hussein, S. N. C. M., Yusuf, S. M., & Japperi, N. S. (2018). Effects of ultrasonic waves during waterflooding for enhanced oil recovery. *International Journal of Engineering and Technology (UAE)*, 7(3), 232–236. <https://doi.org/10.14419/ijet.v7i3.11.16015>
- Fannir, J., Leclerc, S., Panfilova, I., & Stemmelen, D. (2018, September 3–6). *Two-phase displacement in porous media studied by MRI techniques*. [Paper presentation]. ECMOR XVI 2018 - 16th European Conference on the Mathematics of Oil Recovery, Barcelona, Spain. <https://doi.org/10.3997/2214-4609.201802188>
- Fazli-Abukheyli, R., & Darvishi, P. (2019). Combination of axial dispersion and velocity profile in parallel tanks-in-series compartment model for prediction of residence time distribution in a wide range of non-ideal laminar flow regimes. *Chemical Engineering Science*, 195, 531–540. <https://doi.org/10.1016/j.ces.2018.09.052>
- Fen, C.S., Lin, Y.R., & Chen, C.Y. (2020). Methane transport in a soil column: experimental and modeling investigation. *Environmental Engineering Research*, 26(5), 200–311. <https://doi.org/10.4491/eer.2020.311>
- Goswami, S., Pant, H. J., Sheoran, M., Chandra, A., Sharma, V. K., & Bhunia, H. (2020). Residence time distribution measurements in an industrial-scale pulp digester using technetium-99m as radiotracer. *Journal of Radioanalytical and Nuclear Chemistry*, 323(3), 1373–1379. <https://doi.org/10.1007/s10967-019-06730-3>
- Hamidi, H., & Rafati, R. (2012, May 21–22). *Prediction of oil reservoir porosity based on BP-ANN*. [Paper presentation]. ICIMTR 2012 - 2012 International Conference on Innovation, Management and Technology Research, Malacca, Malaysia. <https://doi.org/10.1109/ICIMTR.2012.6236396>
- IAEA. (2001). Radiotracer Technology as Applied to Industry, IAEA-TECDOC-1262.
- IAEA. (2004). Radiotracer Applications in Industry - A Guidebook, Technical Report Series No. 42.
- IAEA. (2008). Radiotracer Residence Time Distribution Method for Industrial and Environmental Applications: Material for Education and On-the-job Training for Practitioners of Radiotracer Technology, Training Course Series No. 31 (Vol. 31). International Atomic Energy Agency. <https://www.iaea.org/publications/7891/radiotracer-residence-time-distribution-method-for-industrial-and-environmental-applications>
- Jegade, A. O., Zeeman, G., & Bruning, H. (2019). Evaluation of liquid and solid phase mixing in Chinese dome digesters using residence time distribution (RTD) technique. *Renewable Energy*, 143, 501–511. <https://doi.org/10.1016/j.renene.2019.04.160>
- Kasban, H., Arafa, H., & Elaraby, S. M. S. (2016). Principle component analysis for radiotracer signal separation. *Applied Radiation and Isotopes*, 112, 20–26. <https://doi.org/10.1016/j.apradiso.2016.03.005>
- Kasban, H., Zahran, O., Arafa, H., El-Kordy, M., Elaraby, S. M. S., & Abd El-Samie, F. E. (2010). Laboratory experiments and modeling for industrial radiotracer applications. *Applied Radiation and Isotopes*, 68(6), 1049–1056. <https://doi.org/10.1016/j.apradiso.2010.01.044>

## Acknowledgement

The authors would like to thank all PAT and UiTM colleagues who have directly and indirectly participated in this work. Special appreciation to the sponsors: IAEA Research Contract No: 22898, IAEA Coordinated Research Project F22069, Fundamental Research Grant Scheme (FRGS) Project No. 600-IRMI/FRGS5/3(085/2019), and Project No. FRGS/1/2018/TK07/MOSTI/02/3 provided by the Ministry of Higher Education Malaysia.

- Lu, K., Chu, J., & Chu, M. (2019). Optimization of RTD-A Controller Parameters Based on Empirical Bat Algorithm. *IOP Conference Series: Materials Science and Engineering*, 569(4), 042023. <https://doi.org/10.1088/1757-899X/569/4/042023>
- Ma, Z., Wang, Y., Ren, N., & Shi, W. (2019). A coupled CFD-DEM simulation of upward seepage flow in coarse sands. *Marine Georesources and Geotechnology*, 37(5), 589–598. <https://doi.org/10.1080/1064119X.2018.1466223>
- Melo, M. A., & Almeida, A. R. (2017, March 15–16). *Determining the sweep efficiency of waterflooding using tracers*. [Paper presentation]. 2017 Society of Petroleum Engineers - SPE Latin America and Caribbean Mature Fields Symposium, Salvador, Bahia, Brazil. <https://doi.org/10.2118/184956-ms>
- Menon, S. H., Madhu, G., & Mathew, J. (2019). Modeling residence time distribution (RTD) behavior in a packed-bed electrochemical reactor (PBER). *International Journal of Chemical Engineering*, 2019. <https://doi.org/10.1155/2019/7856340>
- Mettler, F. A., & Guiberteau, M. J. (2012). Radioactivity, Radionuclides, and Radiopharmaceuticals. In *Essentials of Nuclear Medicine Imaging* (pp. 1–21). Elsevier. <https://doi.org/10.1016/b978-1-4557-0104-9.00001-9>
- Mora, G., Bonfanti, B., Porlles, J., Casas, J., & Agudelo, O. (2016, June 13–15). *Channeling identification: A routine surveillance exercise for successful waterflooding management in Casabe Alliance*. [Paper presentation]. Society of Petroleum Engineers - SPE Trinidad and Tobago Section Energy Resources Conference, Port of Spain, Trinidad and Tobago. <https://doi.org/10.2118/180814-MS>
- Othman, N., Ibrahim, M., Yussup, N., Yussof, N. H., & Syafiq Yunos, M. A. (2018). Application of Smart Radiotracer Data Analysis (SRDA) Software for Industrial Application. *IOP Conference Series: Materials Science and Engineering*, 458(1), 012083. <https://doi.org/10.1088/1757-899X/458/1/012083>
- Othman, N., & Kamarudin, S. K. (2014). Radiotracer technology in mixing processes for industrial applications. In *The Scientific World Journal* (Vol. 2014). Scientific World Ltd. <https://doi.org/10.1155/2014/768604>
- Othman, N., Saaid, I. M., Ahmed, A., Yusof, N. H., Yahya, R., Yunos, M. A. S. M., Chik, E. M. F. E., Shari, M. R., Hassan, H., & Mahmood, A. A. (2020). Investigation of water-flooding activity using radiotracer technology in commercial core-flood set up. *ASEAN Journal of Chemical Engineering*, 20(1), 49–56. <https://doi.org/10.22146/ajche.51902>
- Pinkerton, T. C., Desilets, C. P., Hoch, D. J., Mikelsons, M. V., & Wilson, G. M. (1985). Bioinorganic activity of technetium radiopharmaceuticals. *Journal of Chemical Education*, 62(11), 954–964. <https://doi.org/10.1021/ed062p965>
- Rahmani, O., Aali, J., Junin, R., Mohseni, H., Padmanabhan, E., Azdarpour, A., Zarza, S., Moayyed, M., & Ghazanfari, P. (2013). The origin of oil in the Cretaceous succession from the South Pars Oil Layer of the Persian Gulf. *International Journal of Earth Sciences*, 102(5), 1337–1355. <https://doi.org/10.1007/s00531-012-0855-3>
- Ranamukhaarachchi, S. A., Esposito, T. v., Raeiszadeh, M., Häfeli, U. O., & Stoeber, B. (2019). Precise measurement of intradermal fluid delivery using a low activity technetium-99m pertechnetate tracer. *Vaccine*, 37(51), 7463–7469. <https://doi.org/10.1016/j.vaccine.2019.09.078>
- Rodríguez López, D., Torres Valle, A., Soria Guevara, M. A., & Ayra Pardo, F. E. (2017). Risk analysis applied to the production of generators of Molybdenum-99/Techneium-99m. *Nucleus (Havana)*, 49(23).
- Schölmerich, J., Schmidt, E., Schümichen, C., Billmann, P., Schmidt, H., & Gerok, W. (1988). Scintigraphic assessment of bowel involvement and disease activity in Crohn's disease using technetium 99m-hexamethyl propylene amine oxine as leukocyte label. *Gastroenterology*, 95(5), 1287–1293. [https://doi.org/10.1016/0016-5085\(88\)90363-0](https://doi.org/10.1016/0016-5085(88)90363-0)
- Sheoran, M., Chandra, A., Bhunia, H., Bajpai, P. K., & Pant, H. J. (2018). Residence time distribution studies using radiotracers in chemical industry—A review. In *Chemical Engineering Communications*, 205(6), 739–758. Taylor and Francis Ltd. <https://doi.org/10.1080/00986445.2017.1410478>
- Sievers, D. A., & Stickel, J. J. (2018). Modeling residence-time distribution in horizontal screw hydrolysis reactors. *Chemical Engineering Science*, 175, 396–404. <https://doi.org/10.1016/j.ces.2017.10.012>
- Skuridin, V. S., Chernov, V. I., Sadkin, V. L., Stasyuk, E. S., Varlamova, N. v., Rogov, A. S., Nesterov, E. A., Ilina, E. A., Larionova, L. A., & Medvedeva, A. A. (2016). Factors affecting elution characteristics of sorption generators of technetium-99m. *AIP Conference Proceedings*, 1760(1), 020062. <https://doi.org/10.1063/1.4960281>
- Suekane, T., Ono, J., Hyodo, A., & Nagatsu, Y. (2017). Three-dimensional viscous fingering of miscible fluids in porous media. *Physical Review Fluids*, 2(10), 103902. <https://doi.org/10.1103/PhysRevFluids.2.103902>
- Sugiharto, S., Su'ud, Z., Kurniadi, R., Wibisono, W., & Abidin, Z. (2009). Radiotracer method for residence time distribution study in multiphase flow system. *Applied Radiation and Isotopes*, 67(7–8), 1445–1448. <https://doi.org/10.1016/j.apradiso.2009.02.073>
- Sun, X., Alhuraishawy, A. K., Bai, B., & Wei, M. (2018). Combining preformed particle gel and low salinity waterflooding to improve conformance control in fractured reservoirs. *Fuel*, 221, 501–512. <https://doi.org/10.1016/j.fuel.2018.02.084>
- van der Velden, S., Dietze, M. M. A., Viergever, M. A., & de Jong, H. W. A. M. (2019). Fast technetium-99m liver SPECT for evaluation of the pretreatment procedure for radioembolization dosimetry. *Medical Physics*, 46(1), 345–355. <https://doi.org/10.1002/mp.13253>
- Wojewódka, P., Aranowski, R., & Jungnickel, C. (2019). Residence time distribution in rapid multiphase reactors. *Journal of Industrial and Engineering Chemistry*, 69, 370–378. <https://doi.org/10.1016/j.jiec.2018.09.037>
- Woods, D. A. (1982). *Radiation safety*. [https://inis.iaea.org/search/search.aspx?orig\\_q=RN:14792614](https://inis.iaea.org/search/search.aspx?orig_q=RN:14792614)

- Zhong, Z., Sun, A. Y., Wang, Y., & Ren, B. (2020). Predicting field production rates for waterflooding using a machine learning-based proxy model. *Journal of Petroleum Science and Engineering*, 194, 107574. <https://doi.org/10.1016/j.petrol.2020.107574>
- Zitha, P., Felder, R., Zornes, D., Brown, K., & Mohanty, K. (2011). Increasing Hydrocarbon Recovery Factors. *Society of Petroleum Engineering*